Atmospheric
Chemistry
and Physics
Discussions

Open Access

Ozone changes under solar geoengineering: implications for UV exposure and air quality

P. J. Nowack[1], N. L. Abraham[1,2], P. Braesicke[3], and J. A. Pyle[1,2]

[1]Centre for Atmospheric Science, Department of Chemistry, University of Cambridge, Cambridge, UK
[2]National Centre for Atmospheric Science, UK
[3]Karlsruhe Institute of Technology, IMK-ASF, 76344 Eggenstein-Leopoldshafen, Germany

Correspondence to: P. J. Nowack (pjn35@cam.ac.uk)

Discussion Paper | Discussion Paper | Discussion Paper | Discussion Paper

ACPD

15, 31973–32004, 2015

Ozone changes under solar geoengineering

P. J. Nowack et al.

Title Page

Abstract	Introduction
Conclusions	References
Tables	Figures

|◀ | ▶|
◀ | ▶
Back | Close

Full Screen / Esc

Printer-friendly Version

Interactive Discussion

P. J. Nowack et al.

Title Page

Abstract | Introduction

Conclusions | References

Tables | Figures

|◄ | ►|

◄ | ►

Back | Close

Full Screen / Esc

Printer-friendly Version

Interactive Discussion

Abstract

Various forms of geoengineering have been proposed to counter anthropogenic climate change. Methods which aim to modify the Earth's energy balance by reducing insolation are often subsumed under the term Solar Radiation Management (SRM). Here, we present results of a standard SRM modelling experiment in which the incoming solar irradiance is reduced to offset the global mean warming induced by a quadrupling of atmospheric carbon dioxide. For the first time in an atmosphere–ocean coupled climate model, we include atmospheric composition feedbacks such as ozone changes under this scenario. Including the composition changes, we find large reductions in surface UV-B irradiance, with implications for vitamin D production, and increases in surface ozone concentrations, both of which could be important for human health. We highlight that both tropospheric and stratospheric ozone changes should be considered in the assessment of any SRM scheme, due to their important roles in regulating UV exposure and air quality.

1 Introduction

The scientific consensus (Stocker et al., 2013) is that man-made climate change caused by anthropogenic emissions of greenhouse gases such as carbon dioxide is taking place. However, despite this knowledge, atmospheric carbon dioxide levels are still rising rapidly. Under these circumstances researchers have reopened the discussion on alternative measures to counteract the effects of climate change (e.g. Govindasamy and Caldeira, 2000; Cicerone, 2006; Crutzen, 2006). Such manipulative measures are commonly referred to as *geoengineering*, "the intentional large-scale manipulation of the environment that is intended to reduce undesired anthropogenic climate change" (Keith, 2000).

Here, we use an atmosphere–ocean chemistry-climate model to study atmospheric composition changes for one of the most common geoengineering modelling experi-

ments: the reflection of solar energy before it can enter the Earth's atmosphere, an idea often depicted by the use of space mirrors (Early, 1989; Seifritz, 1989). This idealised geoengineering experiment belongs to methods subsumed under the term Solar Radiation Management (SRM). SRM methods aim to offset the additional radiative forcing due to increases in atmospheric greenhouse gas concentrations by reflecting solar radiation before it can reach the Earth's surface. The central problem with any SRM scheme is that they are not designed to directly address the cause of change, namely the elevated levels of carbon dioxide and other greenhouse gases in the Earth system but, rather, to affect other processes whose changes counteract those due to the greenhouse gases (Shepherd, 2009). This has been demonstrated in numerous SRM modelling studies (e.g. Bala et al., 2008; Govindasamy and Caldeira, 2000; Govindasamy et al., 2002, 2003; Jones et al., 2011; Kravitz et al., 2012, 2013a; Lunt et al., 2008; Matthews and Caldeira, 2007; Niemeier et al., 2013; Ricke et al., 2010; Schmidt et al., 2012; Tilmes et al., 2013).

Atmospheric composition changes under SRM have received much attention in the context of stratospheric particle injection schemes (Budyko, 1977; Crutzen, 2006) as increased particle loadings could enhance the heterogeneous catalysis of reactions that eventually lead to ozone depletion (e.g. Heckendorn et al., 2011; Pitari et al., 2014; Pope et al., 2012; Rasch et al., 2008; Tilmes et al., 2008, 2009, 2012; Weisenstein and Keith, 2015). This would have important implications for human health since ozone is the major absorber of solar UV-B radiation, which interacts with the human DNA and which has been connected to many acute and chronic illnesses of the eye, immune system and skin and, inter alia, to various forms of skin cancer (e.g. Norval et al., 2011; Slaper et al., 1996). However, UV-B radiation is also needed in beneficial biological processes such as in the photobiological production of vitamin D (Holick, 1981). Vitamin D deficiency has been related to an increased likelihood of occurrence of internal cancers, autoimmune diseases, mental illnesses, lower bone density and many more (e.g. Mora et al., 2008; Norval et al., 2011; Ross et al., 2011; Williamson et al., 2014). Therefore, significantly lower surface UV-B could also have considerable adverse effects on

human health or could make lifestyle changes necessary (McKenzie et al., 2009). Similarly, other organisms of the biosphere depend on UV radiation including certain types of plants whose defence mechanisms against pests and pathogenic micro-organisms are regulated by UV-B radiation (Williamson et al., 2014). Another important factor is changes in ozone at the surface, where ozone acts as a pollutant which has been associated both with diseases of the respiratory system and crop damage (Avnery et al., 2011; Silva et al., 2013).

In contrast to the often studied case of particle injection schemes, composition changes and their potential health impacts in a "space-mirror" geoengineered climate have not yet been included in a 3-D atmosphere–ocean modelling study. Here, we investigate changes in ozone, and consequently in biologically active ultraviolet surface radiation (in particular UV-B), contrasting our results with composition changes under pure greenhouse gas forcing. Changes in UV-B fluxes by changes in clouds and surface albedo are also considered. In addition, we discuss potential surface ozone, and thus air quality, changes as a result of SRM.

This paper is organised as follows: Sect. 2.1 and 2.2 introduces the model used to run the simulations and the experimental setup. Section 3.1 introduces the global and regional surface temperature response. Changes in atmospheric composition and their impact on surface UV and air quality are explained in Sect. 3.2 to 3.4. The final Sect. 4 puts our results into context, also regarding other SRM schemes and health implications.

2   Experimental setup

2.1   Model description

A version of the recently developed atmosphere–ocean coupled configuration of the Hadley Centre Global Environment Model version 3, additionally coupled to an atmo-

spheric chemistry scheme, has been employed here (Hewitt et al., 2011; Nowack et al., 2015).

For the atmosphere, the UK Met Office's Unified Model (MetUM) version 7.3 is used. The configuration is based on a regular grid with a horizontal resolution of $3.75°$ longitude by $2.5°$ latitude and comprises 60 vertical levels up to a height of $\sim 84\,\mathrm{km}$, and so includes a full representation of the stratosphere. Its dynamical core is non-hydrostatic and employs a semi-Lagrangian advection scheme. The radiation scheme by Edwards and Slingo (1996) is used in the MetUM with 9 bands in the longwave and 6 bands in the shortwave part of the spectrum. Subgridscale features such as clouds and gravity waves are parameterised.

The ocean component is the Nucleus for European Modelling of the Ocean (NEMO) model version 3.0 coupled to the Los Alamos sea ice model CICE version 4.0. It contains 31 vertical levels reaching down to a depth of $5\,\mathrm{km}$. The NEMO configuration used in this study deploys a tripolar, locally anisotropic grid which has $2°$ resolution in longitude everywhere, but an increased latitudinal resolution in certain regions with up to $0.5°$ in the tropics.

Atmospheric chemistry is represented by the UK Chemistry and Aerosols (UKCA) model in an updated version of the stratospheric chemistry configuration (Morgenstern et al., 2009) which is coupled to the MetUM. A simple tropospheric chemistry scheme that simulates hydrocarbon oxidation is included, which provides for emissions of 3 chemical species (NO (surface, lightning), CO (surface), HCHO (surface)). In addition, surface mixing ratios of 4 further species (N_2O, CH_3Br, H_2, CH_4) are constrained by calculating the effective emission required to maintain their surface mixing ratios, e.g. for nitrous oxide 280 ppbv and for methane 790 ppbv. This keeps their tropospheric mixing ratios constant at approximately pre-industrial levels in all simulations. Nitrogen oxide emissions from lightning are parameterized according to Price and Rind (1992, 1994). Changes in photolysis rates in the troposphere and the stratosphere are calculated interactively using the Fast-JX photolysis scheme (Bian and Prather, 2002; Neu et al., 2007; Telford et al., 2013; Wild et al., 2000).

2.2 The simulations – the GeoMIP G1 experiment

Our simulations follow standards set for the G1 experiment (see Table 1), which was defined as part of the Geoengineering Model Intercomparison Project (GeoMIP) (Kravitz et al., 2011, 2013b). In the G1 experiment the effect of an abrupt quadrupling of atmo-

5 spheric carbon dioxide (CO_2) on the global mean surface temperature is approximately offset by reducing the model's solar constant. This can be thought of as an experiment in which space-mirrors reflect sunlight before it enters the Earth's atmosphere (Early, 1989; Seifritz, 1989). Starting from approximately pre-industrial concentrations with atmospheric CO_2 at $\sim$ 285 ppmv (piControl), we thus carried out, firstly, an abrupt 4×CO_2

10 experiment, in which atmospheric CO_2 is instantaneously quadrupled to $\sim$ 1140 ppmv and, secondly, a G1 type experiment in which the global warming caused by 4×CO_2 was offset by a solar irradiance reduction of 49.0 W m^{-2} ($\sim$ 3.6 %). The radiative forcing in the 4×CO_2 experiment roughly matches the levels attained by the end of the 21st century under the transient RCP8.5 forcing scenario defined for the Coupled Model

15 Intercomparison Project phase 5 (Moss et al., 2010; Taylor et al., 2012). Both experiments were run for 75 years after the CO_2 and solar forcings were imposed. For analysis, we use the last 50 years of each experiment in the following. The highly idealised nature and theoretical simplicity of the G1 experiment allows us to discuss possible unintended consequences of solar geoengineering in an intuitive way. These include

20 changes in composition, UV transmission as well as air quality. While the exact quantification of any changes would be strongly dependent on both forcing scenario and SRM scheme, this study aims to demonstrate in a qualitative way why changes in these metrics are to be expected for any SRM scheme.

Title Page

Abstract | Introduction

Conclusions | References

Tables | Figures

|◄ | ►|

◄ | ►

Back | Close

Full Screen / Esc

Printer-friendly Version

Interactive Discussion

3   Results

3.1   Surface temperature response

The temporal evolution of the global mean surface temperature for all simulations is shown in Fig. 1. As expected, a rapid warming is found in $4\times CO_2$ relative to piControl in response to the abrupt forcing whereas G1 remains (by design) at effectively the same average surface temperature. Changes in atmospheric composition (e.g. ozone) exert an additional radiative forcing which can alter the magnitude of the surface warming response to CO_2 (Nowack et al., 2015) and the amount of solar dimming needed to offset it. For example, we needed an additional solar constant reduction of $1.1\,\mathrm{W\,m}^{-2}$ ($50.1\,\mathrm{W\,m}^{-2}$ instead of $49.0\,\mathrm{W\,m}^{-2}$) to offset the global mean surface warming in experiments where we kept ozone and other chemical species fixed at pre-industrial levels. However, we focus on the interactive chemistry model results here. For the pattern of remaining surface temperature anomalies (Fig. 2) our model yields the characteristic distribution of overcooling in the tropics and warming at high latitudes in G1 (Kravitz et al., 2013a), an effect which can be explained by the proportionally larger impact of reducing insolation on the tropics than on high latitudes (Govindasamy and Caldeira, 2000; Lunt et al., 2008).

3.2   Stratospheric ozone and temperature changes

Figure 3a to d shows latitude-height cross sections of changes in zonal mean ozone mass mixing ratio and zonal mean temperature. We find large increases in ozone in the middle-upper stratosphere (~ 30–$50\,\mathrm{km}$ altitude, Fig. 3a and b) under both $4\times CO_2$ and G1, a ubiquitous feature in chemistry-climate modelling studies (e.g. Oman et al., 2010) with a cooler stratosphere under increased atmospheric CO_2 concentrations (Fels et al., 1980), see Fig. 3c. The ozone increases are well understood and are mainly caused by a slowing of catalytic ozone (O_3) loss reactions

$$X + O_3 \rightarrow XO + O_2 \tag{R1a}$$

$$XO + O \rightarrow X + O_2 \tag{R1b}$$

5 Net: $O + O_3 \rightarrow 2O_2$ (R1)

under cooler stratospheric conditions (Haigh and Pyle, 1982), with the radical species X typically being NO, OH, Cl or Br. In addition, the cooling shifts the ratio between atomic oxygen and ozone towards the latter, which further slows down the rate-determining step (R1b) in the catalytic cycles (Jonsson et al., 2004). Stratospheric cooling due to

10 increased CO_2 persists in G1 and the solar irradiance reduction would, as a single effect, rather further cool the stratosphere (Govindasamy et al., 2003; Braesicke et al., 2011). However, some regions in the stratosphere are actually warmer in G1 than in $4 \times CO_2$ (Fig. 3d). Increased shortwave heating by more ozone, local tropopause height shifts and changes in dynamical heating certainly contribute to this, and importantly so

15 does less longwave cooling as a result of the much lower stratospheric water vapour concentrations (Maycock et al., 2011) in G1, see below.

In spite of the partly warmer stratospheric conditions, the ozone increases in the upper stratosphere are larger in G1 than under $4 \times CO_2$ (compare Fig. 3a to b), see also Jackman and Fleming (2014). In our simulations, the main drivers behind this ad-

20 ditional ozone increase are a significant reduction of stratospheric specific humidity in G1 in combination with reduced abundances of atomic oxygen species at constant pressure levels. Atomic oxygen abundances are decreased in G1 for both ground state $O(^3P)$ and the excited state $O(^1D)$ by ~ 3–8% compared to $4 \times CO_2$ (not shown). These decreases are only observable when pressure levels are used as vertical coordinates instead of height coordinates, see Jonsson et al. (2004). Less abundant atomic oxy-

25 gen at a given atmospheric pressure implies a slowing of Reaction (R1b) and thus reduced ozone loss. In addition, our model yields an ~ 10–20% drier atmosphere for G1 than for piControl, as compared to a much more humid atmosphere in $4 \times CO_2$ (stratosphere wetter by $\sim 30\%$ than pre-industrial). The drier atmosphere under SRM

Ozone changes under solar geoengineering

P. J. Nowack et al.

Title Page

Abstract	Introduction
Conclusions	References
Tables	Figures

Back | Close

Full Screen / Esc

Printer-friendly Version

Interactive Discussion

is part of a weaker hydrological cycle (e.g. Bala et al., 2008; Govindasamy et al., 2003; Kravitz et al., 2013a; Lunt et al., 2008; Matthews and Caldeira, 2007; Ricke et al., 2010; Schmidt et al., 2012; Tilmes et al., 2013, 2009), which gives rise to character-istic reductions in global mean precipitation (see Table 2) and evaporation. The more humid stratosphere under $4\times CO_2$ results in greater production of HO_x species from water vapour and thus more ozone loss via Reactions (R1a) and (R1b) than in G1 (the abundance of OH and HO_2 is $\sim$ 15–25 % smaller in the middle-upper stratosphere in G1). Similarly, higher abundances of nitrogen oxides ($NO_x = NO$, NO_2; $\sim$ 5–13 %) in the upper stratosphere under $4\times CO_2$ also contribute. Changes in other radical species play secondary roles in this experiment (Jackman and Fleming, 2014).

In the tropical lower stratosphere, we find ozone decreases under $4\times CO_2$, which is characteristic for an acceleration of the Brewer–Dobson circulation under CO_2 driven tropospheric warming (Nowack et al., 2015; Shepherd and McLandress, 2011). In re-sponse to solar geoengineering, the residual circulation (not shown) and thus ozone (Fig. 3b) in the tropical lower stratosphere is almost brought back to pre-industrial lev-els. The remaining ozone decreases mainly result from an effect often referred to as "inverse self-healing" of the ozone column (e.g. Haigh and Pyle, 1982; Jonsson et al., 2004; Portmann and Solomon, 2007), in which the increased ozone concentrations in the upper stratosphere allow less shortwave radiation to propagate to lower altitudes. Relative to pre-industrial conditions, this mechanism acts in concert with the (by de-sign) reduced insolation to leave fewer photons of relevant wavelengths to produce ozone in the lower stratosphere. However, these effects are partly compensated by co-incident decreases in ozone losses in G1, mainly due to the lower temperatures and lower HO_x concentrations than in piControl. Overall, the significant changes in strato-spheric ozone have important implications for UV fluxes into the troposphere and to the surface, see Sect. 3.3 and 3.4.

Title Page

Abstract | Introduction

Conclusions | References

Tables | Figures

Back | Close

Full Screen / Esc

Printer-friendly Version

Interactive Discussion

3.3 Tropospheric ozone changes

Tropospheric ozone is an important factor in air quality; it affects human health and ecology, see Sect. 1. Ozone concentrations in the troposphere are controlled by a variety of processes which could be affected by SRM. These include

(i) photochemical processes influenced by changing UV-B (280–315 nm) and UV-A (315–400 nm) fluxes into the troposphere (Madronich et al., 2015; Williamson et al., 2014). High energy photons needed to produce ozone from molecular oxygen ($\lambda < 240$ nm) are absorbed at higher altitudes and tropospheric ozone levels are determined by other mechanisms of ozone production and loss. For example, under clean environmental background conditions, ozone loss and production of the hydroxyl radical OH via

$$O_3 + h\nu \ (\lambda < 328\,\text{nm}) \rightarrow O_2 + O(^1D) \tag{R2a}$$
$$O(^1D) + H_2O \rightarrow 2\,OH \tag{R2b}$$
$$\text{Net: } O_3 + H_2O + h\nu \rightarrow O_2 + 2\,OH \tag{R2}$$

is of prime importance. This reaction pathway is non-linearly dependent on stratospheric ozone changes due to the photons needed in Reaction (R2a) (McKenzie et al., 2011).

(ii) changes in tropospheric concentrations of chemical species involved in the formation of ozone or its depletion, for instance in water vapour and thus in concentrations of a key reactant in loss reactions such as Reaction (R2).

(iii) changes in Stratosphere–Troposphere Exchange (STE) (Holton et al., 1995; Morgenstern et al., 2009; Neu et al., 2014; Zeng et al., 2010), i.e. due to changes in the transport of ozone from the ozone-rich stratosphere into the troposphere. Such changes are strongly coupled to atmospheric dynamics.

In our simulations, there is a global mean surface ozone increase in G1 (+5.0 %) and a decrease in 4×CO$_2$ (−4.2 %), see Table 2. The differences between the runs are to first order determined by processes (i) and (ii). Firstly, UV fluxes into the troposphere

decrease in G1 both due to the greater stratospheric ozone concentrations and the solar irradiance reduction. This reduces ozone loss directly via a reduction in the photolysis Reaction (R2a) which slows Reaction (R2b). Secondly, tropospheric ozone loss is further decreased as a result of the up to 20 % lower tropospheric humidity found under SRM than in piControl, as compared to the much more humid conditions under $4 \times CO_2$, which gives rise to the opposite sign response.

Changes in STE (iii) have a negligible effect on the global mean surface ozone change in G1, see Table 2. Nonetheless, STE can be regionally and seasonally important under $4 \times CO_2$, where surface ozone increases at mid- and high latitudes in the Northern Hemisphere and Southern Hemisphere, see Fig. 4a. These annual mean changes result from increases during the respective winter and spring seasons (not shown), and are thus likely driven by greater STE (increased by ~ 38 %). Similarly, tropospheric ozone and HO_x changes due to greater lightning NO_x emissions contribute under $4 \times CO_2$ (Banerjee et al., 2014; Zeng et al., 2008), but are not a factor in G1, see Table 2. In any case they do not define the sign of the global mean response.

We emphasize that the effect of SRM on tropospheric chemistry is expected to be strongly dependent on the scenario, reference state and geoengineering method used. For example, air pollution by nitrogen oxides could change the relative importance of different chemical mechanisms (Morgenstern et al., 2013; Squire et al., 2014; Tang et al., 2011). In addition, our experimental setup does not allow us to assess the full impact of solar geoengineering on the complex chemical mechanisms happening in the troposphere (Sect. 2.1). Nevertheless, our results demonstrate the potential for substantial changes in tropospheric chemistry and thus air quality in the different climate state created by SRM. Here, we find a particularly strong effect in the tropics, where model surface ozone increases under G1 and decreases under $4 \times CO_2$, amounting to annual mean differences of around 5 ppbv between these two simulations in some regions, compare Fig. 4a and b.

3.4 The effect of column ozone and cloud changes on surface UV-B

UV-B surface fluxes can change for a variety of reasons (Bais et al., 2015; McKenzie et al., 2011). Changes in column ozone have the potential to provide particularly strong contributions since ozone is the only major absorber of UV-B radiation in the atmosphere. As discussed above, SRM could affect column ozone; in G1, we find that relative to piControl the global mean column ozone increased by $\sim 8\%$ compared to only $\sim 4\%$ under $4\times CO_2$, see Fig. 5 and Table 2.

The harmful effect of UV exposure on human skin is commonly measured using the UV-Index (UVI), starting at 0 and with higher UVI equalling greater skin-damaging potential (WHO, 2002). Here, we use the approximate formula of Madronich (2007) to estimate UVI changes in response to the changes in column ozone in $4\times CO_2$ and G1 under clear-sky, unpolluted conditions

$$\text{UVI} \sim 12.5\mu^{2.42}(\Omega/300)^{-1.23} \tag{1}$$

where μ is the cosine of the solar zenith angle and Ω the total vertical ozone column in Dobson Units (DU). As a further approximation, we use monthly and zonal mean values for column ozone, but have updated the solar zenith angle on a daily basis according to the changing solar declination. The resulting UVI is therefore both a function of the changing angle of incidence of the Sun's radiation to the Earth's surface and the seasonally varying column ozone (Fig. 5c and d) at a given location. The UVI found for piControl at noon and relative changes (ΔUVI) for G1 and $4\times CO_2$ in percentages, are shown in Fig. 5e and f, see also Table 2 for global mean differences. In G1, the UVI decreases everywhere during the whole year due to both changes in column ozone and the 3.6 % reduced intensity of the solar radiation. However, the effect of the changes in ozone generally dominates. In particular, during Northern Hemisphere (NH) spring and summer average decreases of 10–20 % are found at NH mid and high latitudes in G1. We caution that percentage changes at high latitudes may be larger, but they occur on much lower background UVI levels. In addition, formula (1) is expected to perform less

well in areas of high surface albedo, as is the case in those regions with widespread occurrences of sea and land-ice (Madronich, 2007). Still, we highlight that further lowered UV irradiance in already light-poor seasons and regions could aggravate medical conditions connected to vitamin D deficiency. We note that vitamin D production exhibits

5   a slightly different sensitivity to certain wavelengths of solar radiation than is assumed in the calculation of the UVI (Fioletov et al., 2009; McKenzie et al., 2009) so that our calculations should again be considered as qualitative.

However, column ozone changes are not the only factor with the potential to change surface UV as a result of climate engineering. Changes in clouds, surface reflectivity

10 (due to surface albedo changes), or aerosols could all significantly affect UV transmission, reflection and scattering. Here, we focus on the impact of ozone and cloud changes, assuming that other changes are small under pre-industrial background conditions. The residual high-latitude warming in G1 (Fig. 2b) implies that albedo changes could play a role, e.g. due to decreases in snow and sea-ice. However, in our model,

15 the higher temperatures do not suffice to trigger statistically significant ice or snow loss under SRM, in agreement with multi-model studies of the G1 experiment (Kravitz et al., 2013a; Moore et al., 2014).

A common way to estimate the average effect of clouds on shortwave (SW) surface radiation is the cloud modification factor (CMF_{SW}). The CMF_{SW} is the total solar

20 irradiance ($W\,m^{-2}$) reaching the Earth's surface at any point (all-sky) divided by its idealised clear-sky value in which any cloud effects are ignored (den Outer et al., 2005). A CMF_{SW} of 1 thus implies that the net cloud effect on surface SW radiation is zero, values larger than 1 imply SW amplification by clouds, values smaller than 1 net reflection of SW radiation by clouds. Figure 6a and b shows differences in the CMF_{SW} for $4\times CO_2$

25 and G1 relative to piControl. Under $4\times CO_2$, the overall pattern of CMF_{SW} changes is in agreement with previous (chemistry-)climate modelling results (Bais et al., 2011, 2015) under greenhouse gas forcing. In G1 (Fig. 6b), the CMF_{SW} is predicted to increase in many regions while decreases are virtually non-existent. Similar cloud changes have been found in previous G1 modelling studies and have been attributed to reductions in

the highly reflective cloud cover at low altitudes (Kravitz et al., 2013a; Schmidt et al., 2012). Consequently, an increase in surface SW radiation from cloud changes is expected in G1, which could partly diminish the ΔUVI due to column ozone changes.

In order to compare the UV effects of the changes in CMF_{SW} and ozone, we use an empirical relationship established by den Outer et al. (2005) and modified by Staiger et al. (2008) to estimate the CMF_{SW}-effect in terms of the UVI at noon. The results are presented in Fig. 6c and d. In G1, the UVI changes by clouds are overall positive. As expected, this is the opposite sign response to the UVI changes induced by ozone. However, the cloud effect is much smaller with percentage increases of only $\sim 1–2\%$ for most latitudes and times. Only during NH summer, between around 40–60° N, are UVI increases of comparable size ($\sim 5\%$) to the decreases by column ozone attained. Indeed, our calculations show that cloud effects are generally small and do not offset ozone-induced UV changes in light-poor seasons, i.e. at times when major problems connected to vitamin D deficiency primarily occur.

In summary, our results imply that differences in column ozone and thus surface UV fluxes represent another example of a change to the climate system that is of importance for human health and lifestyle, but which cannot be offset in a simple manner by proposed SRM methods. Such considerations have to be taken into account when evaluating benefits and risks of possible geoengineering schemes.

4 Discussion and conclusions

Using a coupled atmosphere–ocean chemistry-climate model, we have carried out an idealised SRM experiment in which we offset the effect of quadrupling atmospheric carbon dioxide on the global mean surface temperature by reducing the incoming solar radiation. Although the global mean surface temperature is therefore the same in this geoengineering experiment, other environmental factors change considerably. In particular, we find large changes in atmospheric composition, with an $\sim 8\%$ increase in global mean column ozone. Regionally and seasonally, those increases can be much

larger and give rise to estimated reductions of up to $\sim 20\%$ in local UV-indices. Reduced surface UV in turn could have adverse effects on medical conditions connected to vitamin D deficiency. In contrast, the general decrease in UV radiation is also expected to have beneficial effects such as a reduced likelihood in populations of developing skin cancer. We find that cloud-induced UV changes play a minor role compared with the change in ozone column. A further unintended consequence of the SRM scheme considered here would be a change in tropospheric composition. The main drivers of change are decreases in tropospheric specific humidity as well as a reduced flux of UV-B and UV-A radiation into the troposphere. We note that this could alter the lifetime of the greenhouse gas methane in a geoengineered climate (Holmes et al., 2013; Morgenstern et al., 2013) and thus the amount of solar geoengineering needed to offset the anthropogenic greenhouse gas forcing.

It is important to stress again that the modelled changes in atmospheric composition and air quality are strongly scenario- and SRM scheme-dependent. For instance, for stratospheric particle injection schemes, stratospheric ozone depletion would be a major concern (e.g. Pope et al., 2012). In addition, UV considerations for aerosol schemes are further complicated by UV scattering and absorption by the aerosol particles (Tilmes et al., 2012) as well as aerosol indirect effects (Kuebbeler et al., 2012). The relative importance of all of these factors would in turn be dependent on the geoengineering strategy, e.g. the injection methodology (Kravitz et al., 2012; Niemeier et al., 2011) as well as the amount and type of aerosol used (Ferraro et al., 2011; Pope et al., 2012; Tilmes et al., 2008). Aerosol geoengineering might also affect the stratospheric circulation (Ferraro et al., 2015) with likely changes in STE different than found here for the G1 experiment. Finally, it is also unclear how long-term injections of aerosols into the atmosphere would affect air quality at the surface due to potentially much increased particle pollution. Other important factors that would affect composition include the reduction in ozone depleting substances by the Montreal Protocol, not considered here, or changes in tropospheric ozone precursors.

In conclusion, that stratospheric ozone and surface ozone do change under solar geoengineering is a robust modelling result; their effects on human health and ecology could be considerable. Similarly to the oft-cited problems of continued ocean acidification (Caldeira and Wickett, 2003) and changes in the hydrological cycle under SRM, ozone changes and their effect on surface UV and air quality would have to be expected in a solar geoengineered world. Consequently, we highlight this issue as an important factor to be accounted for in future discussions and evaluations of all SRM methods.

References

Avnery, S., Mauzerall, D. L., Liu, J., and Horowitz, L. W.: Global crop yield reductions due to surface ozone exposure?: 2. Year 2030 potential crop production losses and economic damage under two scenarios of O_3 pollution, Atmos. Environ., 45, 2297–2309, doi:10.1016/j.atmosenv.2011.01.002, 2011.

Bais, A. F., Tourpali, K., Kazantzidis, A., Akiyoshi, H., Bekki, S., Braesicke, P., Chipperfield, M. P., Dameris, M., Eyring, V., Garny, H., Iachetti, D., Jöckel, P., Kubin, A., Langematz, U., Mancini, E., Michou, M., Morgenstern, O., Nakamura, T., Newman, P. A., Pitari, G., Plummer, D. A., Rozanov, E., Shepherd, T. G., Shibata, K., Tian, W., and Yamashita, Y.: Projections of UV radiation changes in the 21st century: impact of ozone recovery and cloud effects, Atmos. Chem. Phys., 11, 7533–7545, doi:10.5194/acp-11-7533-2011, 2011.

Bais, A. F., McKenzie, R. L., Bernhard, G., Aucamp, P. J., Ilyas, M., Madronich, S., and Tourpali, K.: Ozone depletion and climate change: impacts on UV radiation, Photochem. Photobio. S., 14, 19–52, doi:10.1039/C4PP90032D, 2015.

Bala, G., Duffy, P. B., and Taylor, K. E.: Impact of geoengineering schemes on the global hydrological cycle, P. Natl. Acad. Sci. USA, 105, 7664–7669, doi:10.1073/pnas.0711648105, 2008.

Banerjee, A., Archibald, A. T., Maycock, A. C., Telford, P., Abraham, N. L., Yang, X., Braesicke, P., and Pyle, J. A.: Lightning NO_x, a key chemistry–climate interaction: impacts of future climate change and consequences for tropospheric oxidising capacity, Atmos. Chem. Phys., 14, 9871–9881, doi:10.5194/acp-14-9871-2014, 2014.

Bian, H. and Prather, M. J.: Fast-J2: Accurate simulation of stratospheric photolysis in global chemical models, J. Atmos. Chem., 41, 281–296, doi:10.1023/A:1014980619462, 2002.

Braesicke, P., Morgenstern, O., and Pyle, J.: Might dimming the sun change atmospheric ENSO teleconnections as we know them?, Atmos. Sci. Lett., 12, 184–188, doi:10.1002/asl.294, 2011.

Budyko, M. I.: Climatic changes, American Geophysical Union, Washington DC, 1977.

Caldeira, K. and Wickett, M. E.: Oceanography: anthropogenic carbon and ocean pH, Nature, 425, 365, doi:10.1038/425365a, 2003.

Caldeira, K. and Wood, L.: Global and Arctic climate engineering: numerical model studies., Philos. Trans. A. Math. Phys. Eng. Sci., 366, 4039–4056, doi:10.1098/rsta.2008.0132, 2008.

Cicerone, R. J.: Geoengineering: encouraging research and overseeing implementation, Climatic Change, 77, 221–226, doi:10.1007/s10584-006-9102-x, 2006.

Crutzen, P. J.: Albedo enhancement by stratospheric sulfur injections: A contribution to resolve a policy dilemma?, Climatic Change, 77, 211–219, doi:10.1007/s10584-006-9101-y, 2006.

Den Outer, P. N., Slaper, H., and Tax, R. B.: UV radiation in the Netherlands: assessing long-term variability and trends in relation to ozone and clouds, J. Geophys. Res.-Atmos., 110, 1–11, doi:10.1029/2004JD004824, 2005.

Early, J. T.: Space-based solar shield to offset greenhouse effect, JBIS-J. Brit. Interpla., 42, 567–569, 1989.

Edwards, J. M. and Slingo, A.: Studies with a flexible new radiation code. I: Choosing a configuration for a large-scale model, Q. J. Roy. Meteor. Soc., 122, 689–719, doi:10.1002/qj.49712253107, 1996.

Title Page

Abstract | Introduction

Conclusions | References

Tables | Figures

|◀ | ▶|

◀ | ▶

Back | Close

Full Screen / Esc

Printer-friendly Version

Interactive Discussion

Fels, S. B., Mahlman, J. D., Schwarzkopf, M. D., and Sinclair, R. W.: Stratospheric sensitivity to perturbations in ozone and carbon dioxide: radiative and dynamical response, J. Atmos. Sci., 37, 2265–2297, doi:10.1175/1520-0469(1980)037<2265:SSTPIO>2.0.CO;2, 1980.

Ferraro, A. J., Highwood, E. J., and Charlton-Perez, A. J.: Stratospheric heating by potential geoengineering aerosols, Geophys. Res. Lett., 38, 1–6, doi:10.1029/2011GL049761, 2011.

Ferraro, A. J., Charlton-Perez, A. J., and Highwood, E. J.: Stratospheric dynamics and midlatitude jets under geoengineering with space mirrors and sulfate and titania aerosols, J. Geophys. Res.-Atmos., 120, 414–429, doi:10.1002/2014JD022734, 2015.

Fioletov, V. E., McArthur, L. J. B., Mathews, T. W., and Marrett, L.: On the relationship between erythemal and vitamin D action spectrum weighted ultraviolet radiation, J. Photochem. Photobiol. B Biol., 95, 9–16, doi:10.1016/j.jphotobiol.2008.11.014, 2009.

Govindasamy, B. and Caldeira, K.: Geoengineering Earth's radiation balance to mitigate CO_2 induced climate change, Geophys. Res. Lett., 27, 2141–2144, doi:10.1029/1999GL006086, 2000.

Govindasamy, B., Thompson, S., Duffy, P. B., Caldeira, K., and Delire, C.: Impact of geoengineering schemes on the terrestrial biosphere, Geophys. Res. Lett., 29, 14–18, doi:10.1029/2002GL015911, 2002.

Govindasamy, B., Caldeira, K., and Duffy, P. B.: Geoengineering Earth's radiation balance to mitigate climate change from a quadrupling of CO_2, Global Planet. Change, 37, 157–168, doi:10.1016/S0921-8181(02)00195-9, 2003.

Haigh, J. D. and Pyle, J. A.: Ozone perturbation experiments in a two–dimensional circulation model, Q. J. Roy. Meteor. Soc., 108, 551–574, doi:10.1002/qj.49710845705, 1982.

Heckendorn, P., Weisenstein, D., Fueglistaler, S., Luo, B. P., Rozanov, E., Schraner, M., Thomason, L. W., and Peter, T.: The Impact of Geoengineering Aerosols on Stratospheric Temperature and Ozone, Environ. Res. Lett., 4, 045108, doi:10.1088/1748-9326/4/4/045108, 2011.

Hewitt, H. T., Copsey, D., Culverwell, I. D., Harris, C. M., Hill, R. S. R., Keen, A. B., McLaren, A. J., and Hunke, E. C.: Design and implementation of the infrastructure of HadGEM3: the next-generation Met Office climate modelling system, Geosci. Model Dev., 4, 223–253, doi:10.5194/gmd-4-223-2011, 2011.

Holick, M. F.: The Cutaneous Photosynthesis of Previtamin D3: A Unique Photoendocrine System, J. Invest. Dermatol., 77, 51–58, doi:10.1111/1523-1747.ep12479237, 1981.

Holmes, C. D., Prather, M. J., Søvde, O. A., and Myhre, G.: Future methane, hydroxyl, and their uncertainties: key climate and emission parameters for future predictions, Atmos. Chem. Phys., 13, 285–302, doi:10.5194/acp-13-285-2013, 2013.

Holton, J. R., Haynes, P. H., Mcintyre, M. E., Douglass, A. R., Rood, B., and Pfister, L.: Stratosphere–Troposphere Exchange, Rev. Geophys., 33, 403–439, 1995.

Hunter, J. D.: Matplotlib: a 2D graphics environment, Comput. Sci. Eng., 9, 90–95, 2007.

Jackman, C. H. and Fleming, E. L.: Stratospheric ozone response to a solar irradiance reduction in a quadrupled $CO_2$2 environment, Earth's Futur., 2, 331–340, doi:10.1002/2014EF000244, 2014.

Jones, A., Haywood, J., and Boucher, O.: A comparison of the climate impacts of geoengineering by stratospheric SO_2 injection and by brightening of marine stratocumulus cloud, Atmos. Sci. Lett., 12, 176–183, doi:10.1002/asl.291, 2011.

Jonsson, A. I., de Grandpré, J., Fomichev, V. I., McConnell, J. C., and Beagley, S. R.: Doubled CO_2-induced cooling in the middle atmosphere: photochemical analysis of the ozone radiative feedback, J. Geophys. Res.-Atmos., 109, 1–18, doi:10.1029/2004JD005093, 2004.

Keith, D. W.: Geoengineering the Climate: history and Prospect, Annu. Rev. Energ. Env., 25, 245–284, doi:10.1146/annurev.energy.25.1.245, 2000.

Kravitz, B., Robock, A., Boucher, O., Schmidt, H., Taylor, K. E., Stenchikov, G., and Schulz, M.: The Geoengineering Model Intercomparison Project (GeoMIP), Atmos. Sci. Lett., 12, 162–167, doi:10.1002/asl.316, 2011.

Kravitz, B., Robock, A., Shindell, D. T., and Miller, M. A.: Sensitivity of stratospheric geoengineering with black carbon to aerosol size and altitude of injection, J. Geophys. Res., 117, 1–22, doi:10.1029/2011JD017341, 2012.

Kravitz, B., Caldeira, K., Boucher, O., Robock, A., Rasch, P. J., Alterskjær, K., Karam, D. B., Cole, J. N. S., Curry, C. L., Haywood, J. M., Irvine, P. J., Ji, D., Jones, A., Kristjánsson, J. E., Lunt, D. J., Moore, J. C., Niemeier, U., Schmidt, H., Schulz, M., Singh, B., Tilmes, S., Watanabe, S., Yang, S., and Yoon, J. H.: Climate model response from the Geoengineering Model Intercomparison Project (GeoMIP), J. Geophys. Res.-Atmos., 118, 8320–8332, doi:10.1002/jgrd.50646, 2013a.

Kravitz, B., Robock, A., Forster, P. M., Haywood, J. M., Lawrence, M. G., and Schmidt, H.: An overview of the Geoengineering Model Intercomparison Project (GeoMIP), J. Geophys. Res.-Atmos., 118, 13103–13107, doi:10.1002/2013JD020569, 2013b.

Ozone changes under solar geoengineering

P. J. Nowack et al.

Title Page

Abstract | Introduction

Conclusions | References

Tables | Figures

◀ | ▶

◀ | ▶

Back | Close

Full Screen / Esc

Printer-friendly Version

Interactive Discussion

Kuebbeler, M., Lohmann, U., and Feichter, J.: Effects of stratospheric sulfate aerosol geo-engineering on cirrus clouds, Geophys. Res. Lett., 39, 1–5, doi:10.1029/2012GL053797, 2012.

Lunt, D. J., Ridgwell, A., Valdes, P. J., and Seale, A.: Sunshade World: a fully coupled GCM evaluation of the climatic impacts of geoengineering, Geophys. Res. Lett., 35, 2–6, doi:10.1029/2008GL033674, 2008.

Madronich, S.: Analytic formula for the clear-sky UV index, Photochem. Photobiol., 83, 1537–1538, doi:10.1111/j.1751-1097.2007.00200.x, 2007.

Madronich, S., Shao, M., Wilson, S. R., Solomon, K. R., Longstreth, J. D., and Tang, X. Y.: Changes in air quality and tropospheric composition due to depletion of stratospheric ozone and interactions with changing climate: implications for human and environmental health, Photochem. Photobio. S., 14, 149–169, doi:10.1039/C4PP90037E, 2015.

Matthews, H. D. and Caldeira, K.: Transient climate-carbon simulations of planetary geoengi-neering, P. Natl. Acad. Sci. USA, 104, 9949–9954, doi:10.1073/pnas.0700419104, 2007.

Maycock, A. C., Shine, K. P., and Joshi, M. M.: The temperature response to stratospheric water vapour changes, Q. J. Roy. Meteor. Soc., 137, 1070–1082, doi:10.1002/qj.822, 2011.

McKenzie, R. L., Liley, J. B., and Björn, L. O.: UV radiation: balancing risks and benefits, Pho-tochem. Photobiol., 85, 88–98, doi:10.1111/j.1751-1097.2008.00400.x, 2009.

McKenzie, R. L., Aucamp, P. J., Bais, A. F., Björn, L. O., Ilyas, M., and Madronich, S.: Ozone depletion and climate change: impacts on UV radiation, Photochem. Photobio. S., 10, 182–198, doi:10.1039/c0pp90034f, 2011.

Moore, J. C., Rinke, A., Yu, X., Ji, D., Cui, X., Li, Y., Alterskjær, K., Kristjánsson, J. E., Muri, H., Boucher, O., Huneeus, N., Kravitz, B., Robock, A., Niemeier, U., Schulz, M., Tilmes, S., Watanabe, S., and Yang, S.: Arctic sea ice and atmospheric circulation under the GeoMIP G1 scenario, J. Geophys. Res.-Atmos., 119, 567–583, doi:10.1002/2013JD021060, 2014.

Mora, J. R., Iwata, M., and von Andrian, U. H.: Vitamin effects on the immune system: vitamins A and D take centre stage, Nat. Rev. Immunol., 8, 685–698, doi:10.1038/nri2378, 2008.

Morgenstern, O., Braesicke, P., O'Connor, F. M., Bushell, A. C., Johnson, C. E., Osprey, S. M., and Pyle, J. A.: Evaluation of the new UKCA climate-composition model – Part 1: The strato-sphere, Geosci. Model Dev., 2, 43–57, doi:10.5194/gmd-2-43-2009, 2009.

Morgenstern, O., Zeng, G., Abraham, N. L., Telford, P. J., Braesicke, P., Pyle, J. A., Hardi-man, S. C., O'connor, F. M., and Johnson, C. E.: Impacts of climate change, ozone recovery,

Ozone changes under solar geoengineering

P. J. Nowack et al.

Title Page

Abstract	Introduction
Conclusions	References
Tables	Figures

|◄ | ►|

◄ | ►

Back | Close

Full Screen / Esc

Printer-friendly Version

Interactive Discussion

and increasing methane on surface ozone and the tropospheric oxidizing capacity, J. Geophys. Res.-Atmos., 118, 1028–1041, doi:10.1029/2012JD018382, 2013.

Moss, R. H., Edmonds, J. A., Hibbard, K. A., Manning, M. R., Rose, S. K., van Vuuren, D. P., Carter, T. R., Emori, S., Kainuma, M., Kram, T., Meehl, G. A., Mitchell, J. F. B., Nakicenovic, N., Riahi, K., Smith, S. J., Stouffer, R. J., Thomson, A. M., Weyant, J. P., and Wilbanks, T. J.: The next generation of scenarios for climate change research and assessment, Nature, 463, 747–756, doi:10.1038/nature08823, 2010.

Neu, J. L., Prather, M. J., and Penner, J. E.: Global atmospheric chemistry: integrating over fractional cloud cover, J. Geophys. Res.-Atmos., 112, 1–12, doi:10.1029/2006JD008007, 2007.

Neu, J. L., Flury, T., Manney, G. L., Santee, M. L., Livesey, N. J., and Worden, J.: Tropospheric ozone variations governed by changes in stratospheric circulation, Nat. Geosci., 7, 340–344, doi:10.1038/NGEO2138, 2014.

Niemeier, U., Schmidt, H., and Timmreck, C.: The dependency of geoengineered sulfate aerosol on the emission strategy, Atmos. Sci. Lett., 12, 189–194, doi:10.1002/asl.304, 2011.

Niemeier, U., Schmidt, H., Alterskjær, K., and Kristjánsson, J. E.: Solar irradiance reduction via climate engineering: impact of different techniques on the energy balance and the hydrological cycle, J. Geophys. Res.-Atmos., 118, 11905–11917, doi:10.1002/2013JD020445, 2013.

Norval, M., Lucas, R. M., Cullen, A. P., de Gruijl, F. R., Longstreth, J., Takizawa, Y., and van der Leun, J. C.: The human health effects of ozone depletion and interactions with climate change, Photochem. Photobio. S., 10, 199–225, doi:10.1039/C0PP90044C, 2011.

Nowack, P. J., Luke Abraham, N., Maycock, A. C., Braesicke, P., Gregory, J. M., Joshi, M. M., Osprey, A., and Pyle, J. A.: A large ozone-circulation feedback and its implications for global warming assessments, Nat. Clim. Change, 5, 41–45, doi:10.1038/nclimate2451, 2015.

Oman, L. D., Waugh, D. W., Kawa, S. R., Stolarski, R. S., Douglass, A. R., and Newman, P. A.: Mechanisms and feedback causing changes in upper stratospheric ozone in the 21st century, J. Geophys. Res.-Atmos., 115, 1–13, doi:10.1029/2009JD012397, 2010.

Pitari, G., Aquila, V., Kravitz, B., Robock, A., Watanabe, S., Cionni, I., Luca, N. de, Genova, G. di, Mancini, E., and Tilmes, S.: Stratospheric ozone response to sulfate geoengineering: results from the Geoengineering Model Intercomparison Project (GeoMIP), J. Geophys. Res.-Atmos., 119, 2629–2653, doi:10.1002/2013JD020566, 2014.

Pope, F. D., Braesicke, P., Grainger, R. G., Kalberer, M., Watson, I. M., Davidson, P. J., and Cox, R. A.: Stratospheric aerosol particles and solar-radiation management, Nat. Clim. Change, 2, 713–719, doi:10.1038/nclimate1528, 2012.

Portmann, R. W. and Solomon, S.: Indirect radiative forcing of the ozone layer during the 21st century, Geophys. Res. Lett., 34, 1–5, doi:10.1029/2006GL028252, 2007.

Price, C. and Rind, D.: A simple lightning parameterization for calculating global lightning distributions, J. Geophys. Res.-Atmos., 97, 9919–9933, doi:10.1029/92JD00719, 1992.

Price, C. and Rind, D.: Modeling Global Lightning Distributions in a General Circulation Model, Mon. Weather Rev., 122, 1930–1939, doi:10.1175/1520-0493(1994)122<1930:MGLDIA>2.0.CO;2, 1994.

Rasch, P. J., Tilmes, S., Turco, R. P., Robock, A., Oman, L., Chen, C.-C., Stenchikov, G. L., and Garcia, R. R.: An overview of geoengineering of climate using stratospheric sulphate aerosols, Philos. Trans. A. Math. Phys. Eng. Sci., 366, 4007–4037, doi:10.1098/rsta.2008.0131, 2008.

Ricke, K. L., Morgan, M. G., and Allen, M. R.: Regional climate response to solar-radiation management, Nat. Geosci., 3, 537–541, doi:10.1038/ngeo915, 2010.

Robock, A., Oman, L., and Stenchikov, G. L.: Regional climate responses to geoengineering with tropical and Arctic SO_2 injections, J. Geophys. Res.-Atmos., 113, 1–15, doi:10.1029/2008JD010050, 2008.

Ross, A. C., Taylor, C. L., Yaktine, A. L., and Del Valle, H. B.: Institute of Medicine (US): dietary reference intakes for calcium and vitamin D, National Academies Press, 2011.

Schmidt, H., Alterskjær, K., Alterskjær, K., Bou Karam, D., Boucher, O., Jones, A., Kristjánsson, J. E., Niemeier, U., Schulz, M., Aaheim, A., Benduhn, F., Lawrence, M., and Timmreck, C.: Solar irradiance reduction to counteract radiative forcing from a quadrupling of CO2: Climate responses simulated by four earth system models, Earth Syst. Dyn., 3, 63–78, doi:10.5194/esd-3-63-2012, 2012.

Seifritz, W.: Mirrors to halt global warming?, Nature, 340, 603, doi:10.1038/340603a0, 1989.

Shepherd, J. G.: Geoengineering the climate: science, governance and uncertainty, Royal Society, 2009.

Shepherd, T. G. and McLandress, C.: A robust mechanism for strengthening of the Brewer–Dobson circulation in response to climate change: critical-layer control of subtropical wave breaking, J. Atmos. Sci., 68, 784–797, doi:10.1175/2010JAS3608.1, 2011.

Title Page

Abstract | Introduction

Conclusions | References

Tables | Figures

|◄ | ►|

◄ | ►

Back | Close

Full Screen / Esc

Printer-friendly Version

Interactive Discussion

Silva, R. A., West, J. J., Zhang, Y., Anenberg, S. C., Lamarque, J.-F., Shindell, D. T., Collins, W. J., Dalsoren, S., Faluvegi, G., Folberth, G., Horowitz, L. W., Nagashima, T., Naik, V., Rumbold, S., Skeie, R., Sudo, K., Takemura, T., Bergmann, D., Cameron-Smith, P., Cionni, I., Doherty, R. M., Eyring, V., Josse, B., MacKenzie, I. A., Plummer, D., Righi, M., Stevenson, D. S., Strode, S., Szopa, S., and Zeng, G.: Global premature mortality due to anthropogenic outdoor air pollution and the contribution of past climate change, Environ. Res. Lett., 8, 034005, doi:10.1088/1748-9326/8/3/034005, 2013.

Slaper, H., Velders, G. J. M., Daniel, J. S., de Gruijl, F. R., and van der Leun, J. C.: Estimates of ozone depletion and skin cancer incidence to examine the Vienna Convention achievements, Nature, 384, 256–258, doi:10.1038/384256a0, 1996.

Squire, O. J., Archibald, A. T., Abraham, N. L., Beerling, D. J., Hewitt, C. N., Lathière, J., Pike, R. C., Telford, P. J., and Pyle, J. A.: Influence of future climate and cropland expansion on isoprene emissions and tropospheric ozone, Atmos. Chem. Phys., 14, 1011–1024, doi:10.5194/acp-14-1011-2014, 2014.

Staiger, H., den Outer, P. N., Bais, A. F., Feister, U., Johnsen, B., and Vuilleumier, L.: Hourly resolved cloud modification factors in the ultraviolet, Atmos. Chem. Phys., 8, 2493–2508, doi:10.5194/acp-8-2493-2008, 2008.

Stocker, T. F., Qin, D., Plattner, G. K., Tignor, M., Allen, S. K., Boschung, J., Nauels, A., Xia, Y., Bex, B., and Midgley, B. M.: IPCC, 2013: Climate Change 2013: the Physical Science Basis. Contribution of working group I to the Fifth Assessment Report of the Intergovernmental Panel on Climate Change, Geneva, Switzerland, 2013.

Tang, X., Wilson, S. R., Solomon, K. R., Shao, M., and Madronich, S.: Changes in air quality and tropospheric composition due to depletion of stratospheric ozone and interactions with climate, Photochem. Photobio. S., 10, 280–291, doi:10.1039/c0pp90039g, 2011.

Taylor, K. E., Stouffer, R. J., and Meehl, G. A.: An overview of CMIP5 and the experiment design, B. Am. Meteorol. Soc., 93, 485–498, doi:10.1175/BAMS-D-11-00094.1, 2012.

Telford, P. J., Abraham, N. L., Archibald, A. T., Braesicke, P., Dalvi, M., Morgenstern, O., O'Connor, F. M., Richards, N. A. D., and Pyle, J. A.: Implementation of the Fast-JX Photolysis scheme (v6.4) into the UKCA component of the MetUM chemistry-climate model (v7.3), Geosci. Model Dev., 6, 161–177, doi:10.5194/gmd-6-161-2013, 2013.

Tilmes, S., Müller, R., and Salawitch, R.: The sensitivity of polar ozone depletion to proposed geoengineer ing schemes, Science, 320, 12011204, doi:10.1126/science.1153966, 2008.

Title Page

Abstract   Introduction

Conclusions   References

Tables   Figures

◄   ►

◄   ►

Back   Close

Full Screen / Esc

Printer-friendly Version

Interactive Discussion

Tilmes, S., Garcia, R. R., Kinnison, D. E., Gettelman, A., and Rasch, P. J.: Impact of geoengi-
neered aerosols on the troposphere and stratosphere, J. Geophys. Res.-Atmos., 114, 1–22,
doi:10.1029/2008JD011420, 2009.

Tilmes, S., Kinnison, D. E., Garcia, R. R., Salawitch, R., Canty, T., Lee-Taylor, J., Madronich, S.,
and Chance, K.: Impact of very short-lived halogens on stratospheric ozone abundance
and UV radiation in a geo-engineered atmosphere, Atmos. Chem. Phys., 12, 10945–10955,
doi:10.5194/acp-12-10945-2012, 2012.

Tilmes, S., Fasullo, J., Lamarque, J. F., Marsh, D. R., Mills, M., Alterskjær, K., Muri, H., Kristjáns-
son, J. E., Boucher, O., Schulz, M., Cole, J. N. S., Curry, C. L., Jones, A., Haywood, J.,
Irvine, P. J., Ji, D., Moore, J. C., Karam, D. B., Kravitz, B., Rasch, P. J., Singh, B., Yoon, J. H.,
Niemeier, U., Schmidt, H., Robock, A., Yang, S., and Watanabe, S.: The hydrological impact
of geoengineering in the Geoengineering Model Intercomparison Project (GeoMIP), J. Geo-
phys. Res.-Atmos., 118, 11036–11058, doi:10.1002/jgrd.50868, 2013.

Weisenstein, D. K., Keith, D. W., and Dykema, J. A.: Solar geoengineering using solid aerosol in
the stratosphere, Atmos. Chem. Phys., 15, 11835–11859, doi:10.5194/acp-15-11835-2015,
2015.

WHO (World Health Organization): Global Solar UV Index, Publication WHO/SDE/OEH/02.2.,
28 pp, Geneva, Switzerland, 2002.

Wild, O., Zhu, X., and Prather, M. J.: Fast-J: accurate simulation of in- and below-
cloud photolysis in tropospheric chemical models, J. Atmos. Chem., 37, 245–282,
doi:10.1023/A:1006415919030, 2000.

Williamson, C. E., Zepp, R. G., Lucas, R. M., Madronich, S., Austin, A. T., Ballare, C. L., Nor-
val, M., Sulzberger, B., Bais, A. F., McKenzie, R. L., Robinson, S. A., Hader, D.-P., Paul, N. D.,
and Bornman, J. F.: Solar ultraviolet radiation in a changing climate, Nat. Clim. Change, 4,
434–441, doi:10.1038/NCLIMATE2225, 2014.

Zeng, G., Pyle, J. A., and Young, P. J.: Impact of climate change on tropospheric ozone and its
global budgets, Atmos. Chem. Phys., 8, 369–387, doi:10.5194/acp-8-369-2008, 2008.

Zeng, G., Morgenstern, O., Braesicke, P., and Pyle, J. A.: Impact of stratospheric ozone
recovery on tropospheric ozone and its budget, Geophys. Res. Lett., 37, L09805,
doi:10.1029/2010GL042812, 2010.

Table 1. Overview of the simulations.

Run	Carbon dioxide (ppmv)	Solar constant reduction ($\mathrm{W\,m^{-2}}$)
piControl	285	–
$4\mathrm{xCO_2}$	1140	–
G1	1140	49.0

Title Page

Abstract | Introduction

Conclusions | References

Tables | Figures

|◀ | ▶|

◀ | ▶

Back | Close

Full Screen / Esc

Printer-friendly Version

Interactive Discussion

Table 2. Global annual mean quantities. For piControl and corresponding differences under $4 \times CO_2$ and G1. The clear-sky, unpolluted UV index at noon is calculated using the formula by Madronich (2007), including only changes by column ozone and by the solar irradiance reduction.

	piControl	$4 \times CO_2$	G1
Surface temperature (K)	288.27	+4.80	−0.02
Precipitation (mm day^{-1})	3.09	+0.19	−0.15
Surface ozone vmr (ppbv)	12.0	−0.5	+0.6
LNO$_x$ emissions (Tg N yr^{-1})	6.2	+3.6	−0.2
STE O$_3$ (Tg yr^{-1})	456	+172	−7
Column ozone (DU)	305.70	+12.85	+23.57
UV index	7.93	−0.07	−0.79

Figure 1. Temporal evolution of the annual and global mean surface temperature anomalies. The anomalies (˚C) are shown relative to the average temperature of the pre-industrial experiment. The piControl and G1 experiment are highlighted in the inset panel with the straight lines marking the average temperature anomalies. The grey and red shading give the ±2σ temperature interval for piControl and G1 respectively.
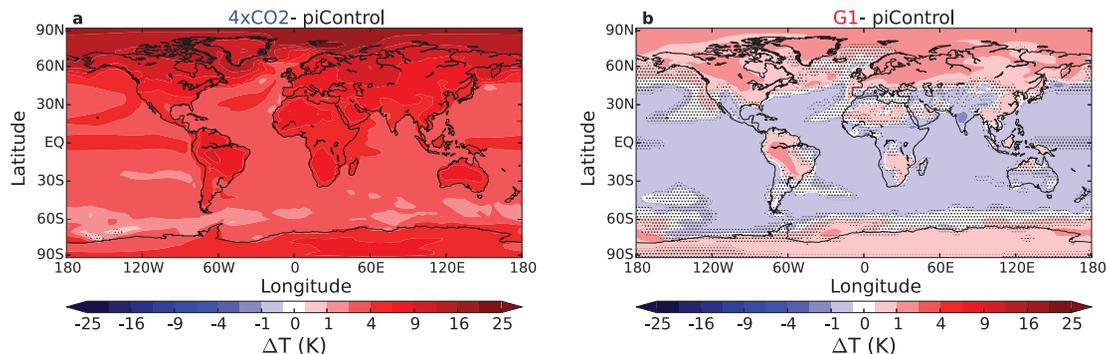
Figure 2. Annual mean surface temperature differences. The differences are based on the average temperatures of the last 50 years of each experiment. **(a)** $4 \times CO_2$ relative to preindustrial conditions. **(b)** G1 relative to pre-industrial conditions. Note the non-linear colour scale. Non-significant changes (using a two-tailed Student's t test at the 95 % confidence level) are marked by stippling.

Title Page

Abstract | Introduction

Conclusions | References

Tables | Figures

|◄ | ►|

◄ | ►

Back | Close

Full Screen / Esc

Printer-friendly Version

Interactive Discussion
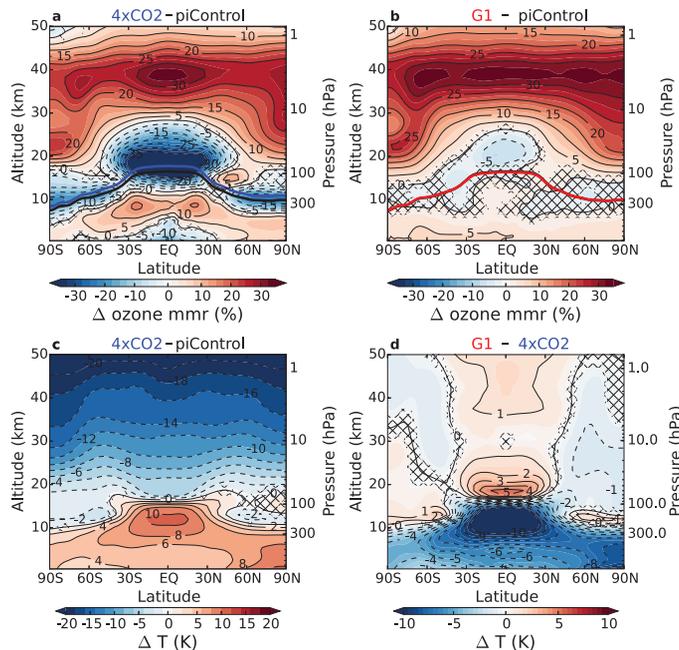
Figure 3. Differences in zonal and annual mean ozone mass mixing ratio and temperature. **(a)**, **(b)** Percentage differences in ozone as labelled. **(c)**, **(d)** Temperature differences (K) as labelled. The ozone changes are given in percentages to highlight the in terms of absolute mass mixing ratios much smaller changes in the ozone-poor troposphere as compared to the larger absolute changes in the stratosphere, which in turn occur on much higher background ozone levels. The colour scale for ozone is adapted to changes in the middle-upper stratosphere; for the whole extent of the changes in the tropical upper troposphere and lower stratosphere under 4×CO_2, see Nowack et al. (2015). Differences are calculated on altitude levels, the pressure axis gives approximate values for pre-industrial conditions. Coloured lines in **(a)**, **(b)** mark the zonal and annual mean tropopause heights for each experiment. Non-significant differences (using a two-tailed Student's t test at the 95 % confidence level) are crossed out.

Title Page

Abstract | Introduction

Conclusions | References

Tables | Figures

|◀ | ▶|

◀ | ▶

Back | Close

Full Screen / Esc

Printer-friendly Version

Interactive Discussion
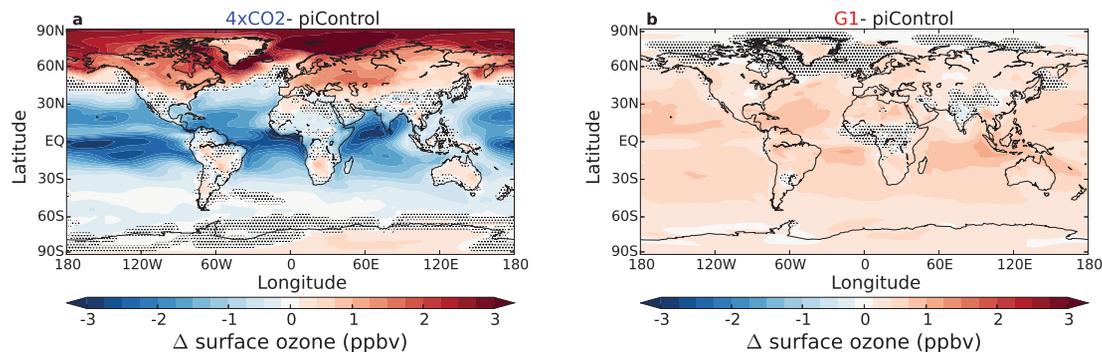
Figure 4. Annual mean surface ozone changes. Absolute values (ppbv). Difference between **(a)** $4\times CO_2$ and piControl, **(b)** G1 and piControl. Non-significant changes (using a two-tailed Student's t test at the 95 % confidence level) are marked by stippling.

Ozone changes under solar geoengineering

P. J. Nowack et al.

Figure 5. Column ozone differences and their impact on the UV index. Relative to piControl: left for 4×CO$_2$, right for G1. Top row: annual mean Δ column ozone (colours, %). Non-significant changes (using a two-tailed Student's t test at the 95 % confidence level) are marked by stippling. Middle row: seasonal cycle of the column ozone changes as longitudinal and monthly means. Bottom row: seasonal cycle of the column ozone induced changes in the UV-index, and in **(f)** additionally by the solar constant reduction, at noon. Polar night regions in **(e)**, **(f)** are crossed out; both daily (solar declination) and monthly changes (ozone) are considered, giving rise to a less smooth appearance. Contour lines show pre-industrial column ozone in Dobson Units (DU) in the upper two rows and pre-industrial UV-indices in the last row.
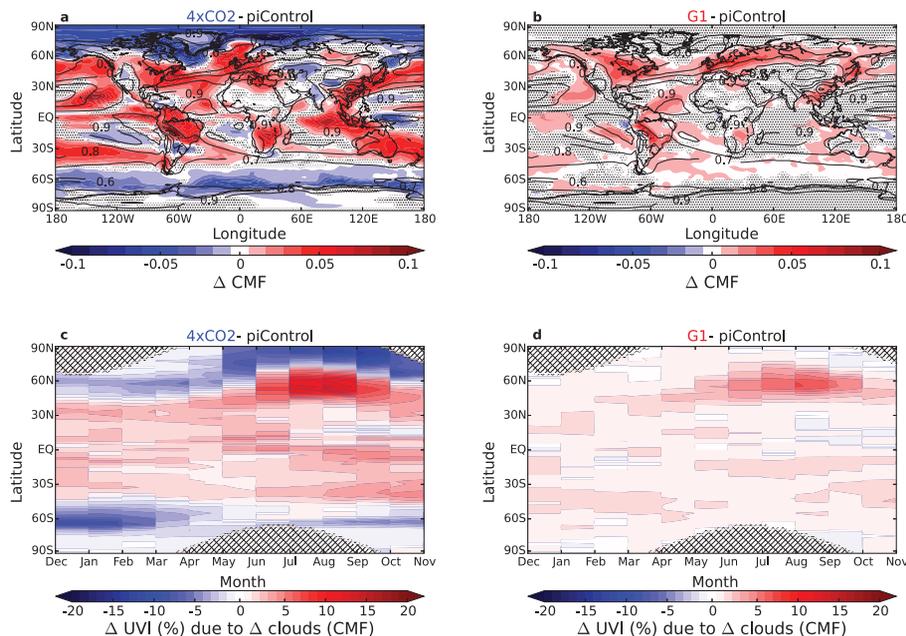
Figure 6. Differences in the cloud modification factor and their impact on the UV index. **(a)** Annual mean ΔCMF (colours) under $4 \times CO_2$ and **(b)** under G1 relative to piControl (contour lines). Non-significant changes (using a two-tailed Student's t test at the 95 % confidence level) are marked by stippling. Zonal mean percentage changes in the UV-index at noon induced by ΔCMF are shown for **(c)** $4 \times CO_2$ and **(d)** G1 according to the formulas by den Outer et al. (2005) and Staiger et al. (2008). Polar night regions in **(c)**, **(d)** are crossed out; both daily (solar declination) and monthly changes (ozone) are considered, giving rise to a less smooth appearance.